iScience

CellPress
OPEN ACCESS

Article

Activating FcγR function depends on endosomal-signaling platforms

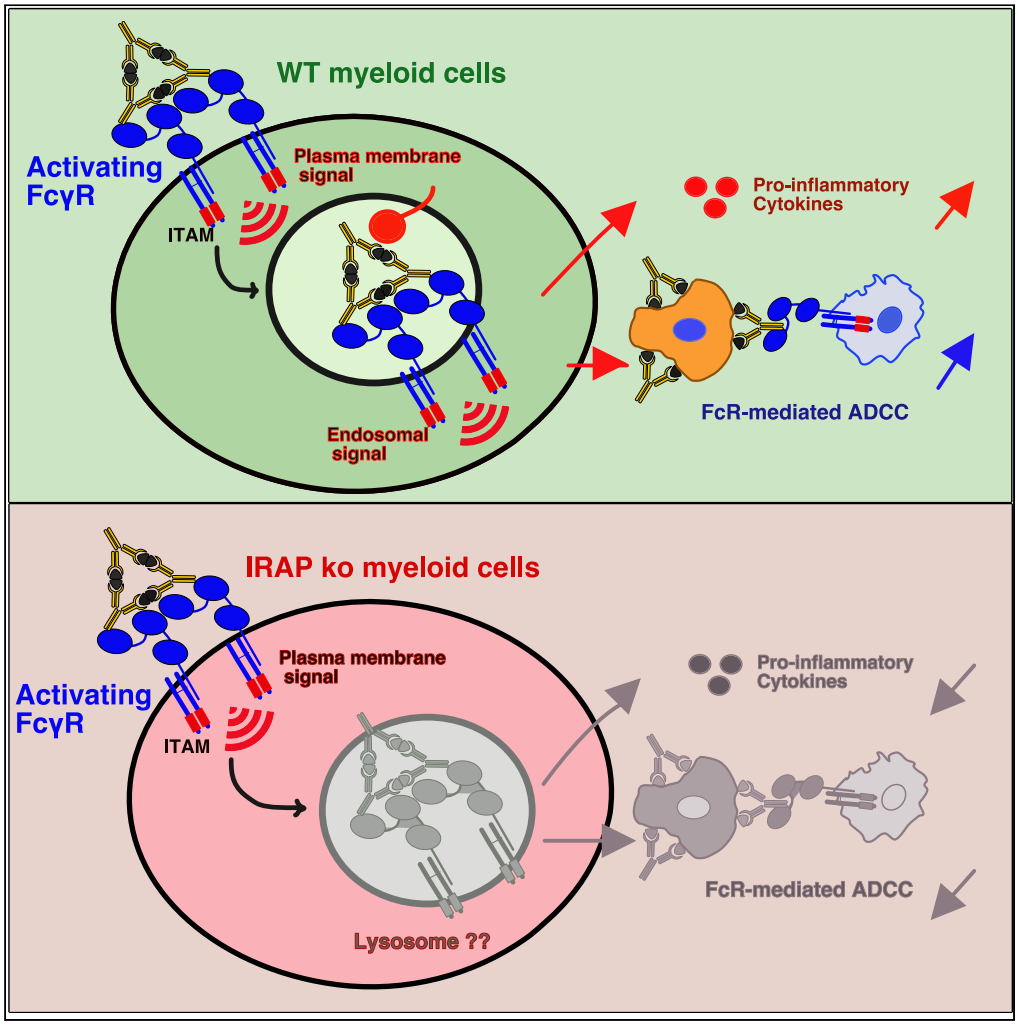

Samira Benadda, Mathilde Nugue, Despoina Koumantou, ..., Renato C. Monteiro, Irini Evnouchidou, Loredana Saveanu

irini.evnouchidou@inovarion.com (I.E.)
loredana.saveanu@inserm.fr (L.S.)

Highlights

Activated IgG receptors FcγRI and FcγRIIA are retained in IRAP^{+} endosomes

Activated IgA receptor FcαRI is targeted to lysosomes

At the endosomal level FcγRI is associated with the Syk, LAT, and PLCγ signaling proteins

IRAP deletion compromises FcγR-mediated cytokine secretion and ADCC

Benadda et al., iScience 26, 107055
July 21, 2023
https://doi.org/10.1016/j.isci.2023.107055

iScience

CellPress
OPEN ACCESS

Article

Activating FcγR function depends on endosomal-signaling platforms

Samira Benadda,[1,2,3,4,9] Mathilde Nugue,[1,2,3,4,9] Despoina Koumantou,[1,2,3,4] Marcelle Bens,[1,2,3,4] Mariacristina De Luca,[1,2,3,4,8] Olivier Pellé,[5,6] Renato C. Monteiro,[1,2,3,4] Irini Evnouchidou,[1,2,3,4,7,*] and Loredana Saveanu[1,2,3,4,10,*]

SUMMARY

Cell surface receptor internalization can either terminate signaling or activate alternative endosomal signaling pathways. We investigated here whether endosomal signaling is involved in the function of the human receptors for Fc immunoglobulin fragments (FcRs): FcαRI, FcγRIIA, and FcγRI. All these receptors were internalized after their cross-linking with receptor-specific antibodies, but their intracellular trafficking was different. FcαRI was targeted directly to lysosomes, while FcγRIIA and FcγRI were internalized in particular endosomal compartments described by the insulin esponsive minoeptidase (IRAP), where they recruited signaling molecules, such as the active form of the kinase Syk, PLCγ and the adaptor LAT. Destabilization of FcγR endosomal signaling in the absence of IRAP compromised cytokine secretion downstream FcγR activation and macrophage ability to kill tumor cells by antibody-dependent cell-mediated cytotoxicity (ADCC). Our results indicate that FcγR endosomal signaling is required for the FcγR-driven inflammatory reaction and possibly for the therapeutic action of monoclonal antibodies.

INTRODUCTION

Cell surface receptors detect signals from the environment and trigger signaling cascades, which usually start at the plasma membrane. From there, the ligand-receptor complexes are internalized, and this internalization was considered until recently as a way to attenuate or terminate the signaling through degradation of the involved proteins. This view changed when it was discovered that endocytosis of the epidermal growth factor receptor (EGFR), that belongs to receptor tyrosine kinases (RTKs), sustains regulated signal transduction from endosomal compartments[1] instead of ending signaling. Later studies showed that many other RTKs and G protein-coupled receptors (GPCRs) are able to signal from endosomes.[2]

In the immune system, the concept of endosomal signaling was described for endosomal toll-like receptors (TLRs)[3] and more recently, it was also shown to apply to the antigen T cell receptor (TCR).[4–6] The ability of the TCR to associate with signaling molecules inside endosomes was first demonstrated using TCR signaling FRET reporters in 2010.[5] Later on, a role of endosomal signaling in TCR function was suggested by the study of T cells deficient for dynamin-2, a protein involved in generation of endocytic vesicles. These cells, despite increased TCR levels at the cell surface, showed reduced proliferation upon TCR activation.[6] More recently, we identified insulin-esponsive aminoPepptidase (IRAP) as a specific marker of TCR signaling endosomes and showed that endosomal TCR signaling is essential for anti-tumor T cell response and T cell survival in the periphery.[4]

The main TCR unit involved in endosomal signaling, the CD3ζ chain, has a high similarity with the γ-chain of receptors for Fc immunoglobulin fragments (FcRs). This homology allows the FcR γ-chain to substitute the CD3ζ chain function in its absence and vice-versa.[7,8] Based on the similar sequence and domain organization of the CD3ζ chain and the FcR γ-chain, we wondered if, similarly to the TCR, the FcRs could also use endosomal signaling platforms.

Most FcRs are activating receptors and, as in the case of the TCR, FcRs signaling is initiated by the phosphorylation of immunoreceptor tyrosine-based activatory motifs (ITAMs). In general, the ITAM is provided

[1]INSERM U1149, CRI, Centre de Recherche sur l'Inflammation, Paris, France

[2]CNRS ERL8252, Paris, France

[3]Université de Paris, Site Xavier Bichat, Paris, France

[4]Inflamex Laboratory of Excellence, Paris, France

[5]INSERM UMR 1163, Cell Sorting Facility, Paris, France

[6]INSERM UMR 1163, Laboratoire of Immunogenetics of Pediatric Autoimmunity, Paris, France

[7]Inovarion, Paris, France

[8]Present address: Evox Therapeutics Limited, Oxford Science Park, Robert Robinson Avenue Oxford OX4 4HG

[9]These authors contributed equally

[10]Lead contact

*Correspondence: irini.evnouchidou@inovarion.com (I.E.), loredana.saveanu@inserm.fr (L.S.)

https://doi.org/10.1016/j.isci.2023.107055

by the γ-chain of FcRs that associates with the α-chain. An exception is the human activating FcγRIIA, which includes an ITAM-like motif in its own cytosolic tail. After ligand binding, ITAMs are phosphorylated by Src-kinases, which allow the binding of the Syk-kinase to the receptor. Once bound to phosphorylated ITAMs, Syk changes its conformation to an open active form. Active Syk is able to autophosphorylate itself on multiple tyrosine residues and activates downstream signaling proteins, such as the LAT adaptor that is a docking site for PLCγ, VAV, and SLP76. In addition to its autophosphorylation, active Syk is also able to phosphorylate the ITAM tyrosine of the receptor, providing thus a positive feedback loop for FcγR signaling.[9] Signaling via activating FcRs is counteracted by the inhibitory receptor FcγRIIB, which contains in its cytosolic tail an immunoreceptor tyrosine-based inhibitory motif (ITIM). When phosphorylated, the ITIM recruits the SHIP and SHP phosphatases that block the propagation of the signal from an activating receptor.[10] Although FcR internalization after immune complex (IC) binding is well documented, the intracellular localization of FcR signaling has not been investigated yet. Thus, it is not known if activated FcRs spend time in the endocytic pathway following their activation or are directly targeted to degradation. To answer this question, we explored the trafficking of FcγRI, FcγRIIA and FcαRI after receptor cross-linking and demonstrate that the activating receptors for IgG have the ability to build endosomal-signaling platforms, which, similar to the TCR, depend on IRAP. IRAP deletion led to decreased FcγR endosomal signaling and FcR-mediated processes, such as proinflammatory cytokine production and antibody-dependent cellular cytotoxicity (ADCC).

RESULTS

Activated FcγRI, FcγRIIA and FcαRI receptors follow distinct trafficking pathways

To obtain a large view of FcR trafficking, we investigated three activating FcRs: FcγRI, a high affinity IgG receptor associated with the γ-chain, FcγRIIA, a low affinity IgG receptor that does not need association with the γ-chain for signaling and FcαRI, an IgA receptor that also associates with the γ-chain. We expressed these receptors as GFP-fusion proteins in the GM-CSF DC-like murine cell line DC2.4. To evaluate the intracellular trafficking of the receptors, we used the early endosomal antigen 1 (EEA1), which is a marker of early endosomes, the TGN38, a marker of trans-Golgi vesicles (TGN), the lysosome marker LAMP1 and IRAP, the marker of specialized, slow recycling storage endosomes known to regulate TLR9[3] and TCR signaling.[4]

To activate FcγRI, the receptor was crosslinked with anti-FcγRI antibodies, and its localization was monitored by immunofluorescence. If in basal conditions FcγRI was localized mainly at the plasma membrane, as early as 15 min after crosslinking, the receptor was not found in EEA1+ early endosomes (Figure 1A) but mainly in IRAP$^+$ endosomes (Figure 1B) and TGN38$^+$ vesicles (Figure S1). Although we did not directly co-stain IRAP and TGN38, they probably colocalize, as previously demonstrated.[11] Half of the receptor and the crosslinking antibodies were retained for more than 60 min in IRAP-TGN38 endosomes, as estimated by quantitative analysis of microscopy images. At 2 h, the last analyzed time point, the receptor accumulated in LAMP1$^+$ lysosomes (Figure 1C).

Similar to FcγRI, FcγRIIA was also internalized in IRAP$^+$ endosomes (Figure 2B), where the receptor-ligand concentration peaked at 30 min and was later targeted to LAMP1$^+$ lysosomes (Figure 2C), probably via EEA1$^+$ endosomes (Figure 2A). Since two different FcγRs were internalized in IRAP$^+$ endosomes, we wanted to investigate whether this intracellular trafficking is specific to IgG receptors, or applies to all activating FcRs. To answer this question, we investigated the trafficking of the FcαRI receptor after crosslinking with the specific antibody A77.[12] In contrast to the behavior of both IgG receptors, FcαRI showed only a very brief transit but did not accumulate in IRAP vesicles and was targeted to lysosomes (Figures 3A–3C).

We conclude that IgG receptors are internalized in IRAP$^+$ endosomes, where their amount is significant until 60 min after activation. In contrast, FcαRI was rapidly targeted to lysosomes. Since the A77 antibody used to crosslink FcαRI binds to the extracellular domain (EC) 2 of FcαRI, while the IgA binding site is located in the EC1 domain of FcαRI,[13] we investigated the receptor trafficking in a more physiological situation. Therefore, we activated FcαRI by IC containing human IgA. However, in this physiological condition, the receptor still showed the same rapid targeting to lysosomes (Figure S2). These results indicate that intracellular trafficking of IgG and IgA Fc receptors is different.

Activated FcγRI recruits several signaling partners in IRAP endosomes

Since FcγRI was the receptor with the longest retention in IRAP endosomes, we wondered if, similar to the TCR,[4] FcγRI is able to signal from this location. As a first approach to investigate endosomal signaling, we

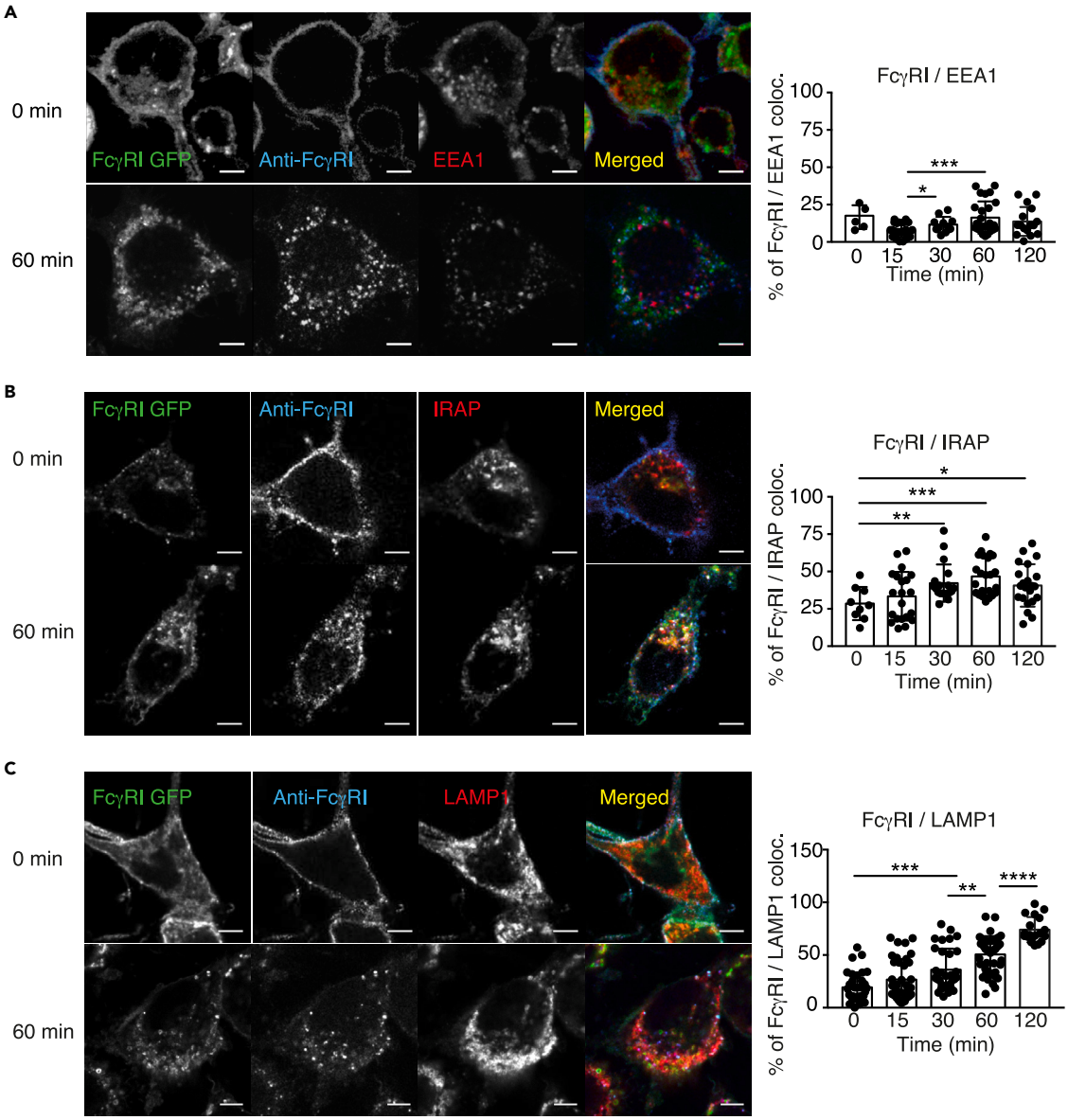

Figure 1. Activated FcγRI is retained in intracellular compartments described by IRAP

(A–C) DC2.4 cells expressing FcγRI-GFP (green) were incubated with anti-FcγRI (clone 10.1) and cross-linked with anti-mouse IgG (blue) at 4°C. After removal of excess antibodies, the cells were shifted for the indicated time points at 37°C, fixed and stained for EEA1 (red) (A), IRAP (red) (B) or LAMP1 (red) (C). The pictures show representative images from three independent experiments and the graphs show colocalization between FcγRI and the endocytic markers. Each dot represents a cell. Data are represented as mean ± SEM. Scale bars = 5 μm. *p < 0.05; **p < 0.01; ***p < 0.001; ****p < 0.0001.

analyzed the colocalization between the receptor and the main components of the FcγR signalosome, in basal conditions and after cell stimulation by receptor cross-linking. In basal conditions, 20% of total pSrc colocalized with IRAP, both at the plasma membrane, but also in endosomes labeled by IRAP (Figure 4A). After receptor activation, pSrc colocalization with IRAP increased to 50% and remained stable for 30 min, before decreasing to 30% at 2 h (Figure 4A). Not only pSrc, but also other components of FcγR signalosomes, such as LAT (Figure 4B) and PLCγ (Figure 4C) showed a similar colocalization with IRAP after receptor activation.

The presence of these signaling proteins in IRAP$^+$ vesicles, was probably due to their association with FcγRI, which was massively internalized in IRAP$^+$ endosomes (Figure 4D). Endosomal association of FcγRI with the signalosome components was also suggested by the colocalization of activated FcγRI with pSrc,

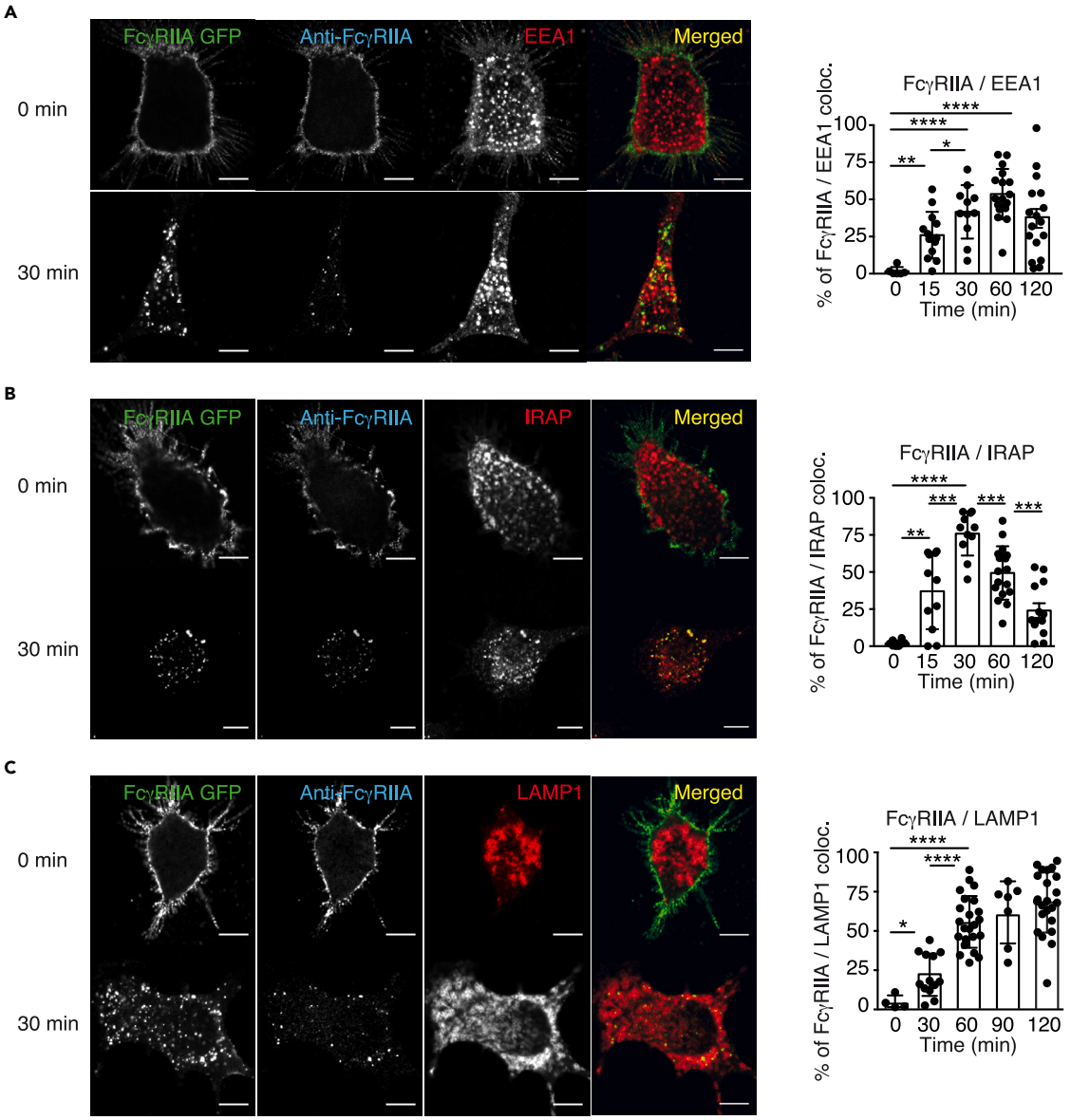

Figure 2. Activated FcγRIIA shows a dynamic passage through IRAP endosomes

(A–C) DC2.4 cells expressing FcγRIIA-GFP (green) were incubated with anti-FcγRIIA (clone IV.3) and cross-linked with anti-mouse IgG (blue) at 4°C. After removal of excess antibodies, the cells were shifted for the indicated time points at 37°C, fixed and stained for EEA1 (red) (A), IRAP (red) (B) or LAMP1 (red) (C). The pictures show representative images from three independent experiments and the graphs show colocalization between FcγRIIA and the endocytic markers. Each dot represents a cell. Data are represented as mean ± SEM. Scale bars = 5 μm. *p < 0.05; **p < 0.01; ***p < 0.001; ****p < 0.0001.

LAT, PLCγ (Figure S3A), and pSyk (Figure S3B), as well as by the co-immunoprecipitation experiments showing that FcγRI pulled down IRAP, pSyk, and PLCγ. The most efficient co-immunoprecipitation was observed at 60 min after receptor cross-linking (Figure S3C).

Such a strong colocalization of activated FcR with signaling proteins at late time points was unexpected. To confirm these findings, we used an alternative method to investigate protein interactions *in situ* by FRET-FLIM (Fluorescence Resonance Energy Transfer—Fluorescence Lifetime IMaging). To investigate FcγRI interaction with Syk, we expressed FcγRI-GFP and Syk-mCherry in DC2.4 cells (Figure S3D) and measured the lifetime of GFP in steady state and after receptor cross-linking. The shortest GFP lifetime, which is equivalent to the strongest interaction between FcγRI-GFP and Syk-mCherry, was observed at 60 min after receptor cross-linking (Figure 4E). This result, together with the microscopy

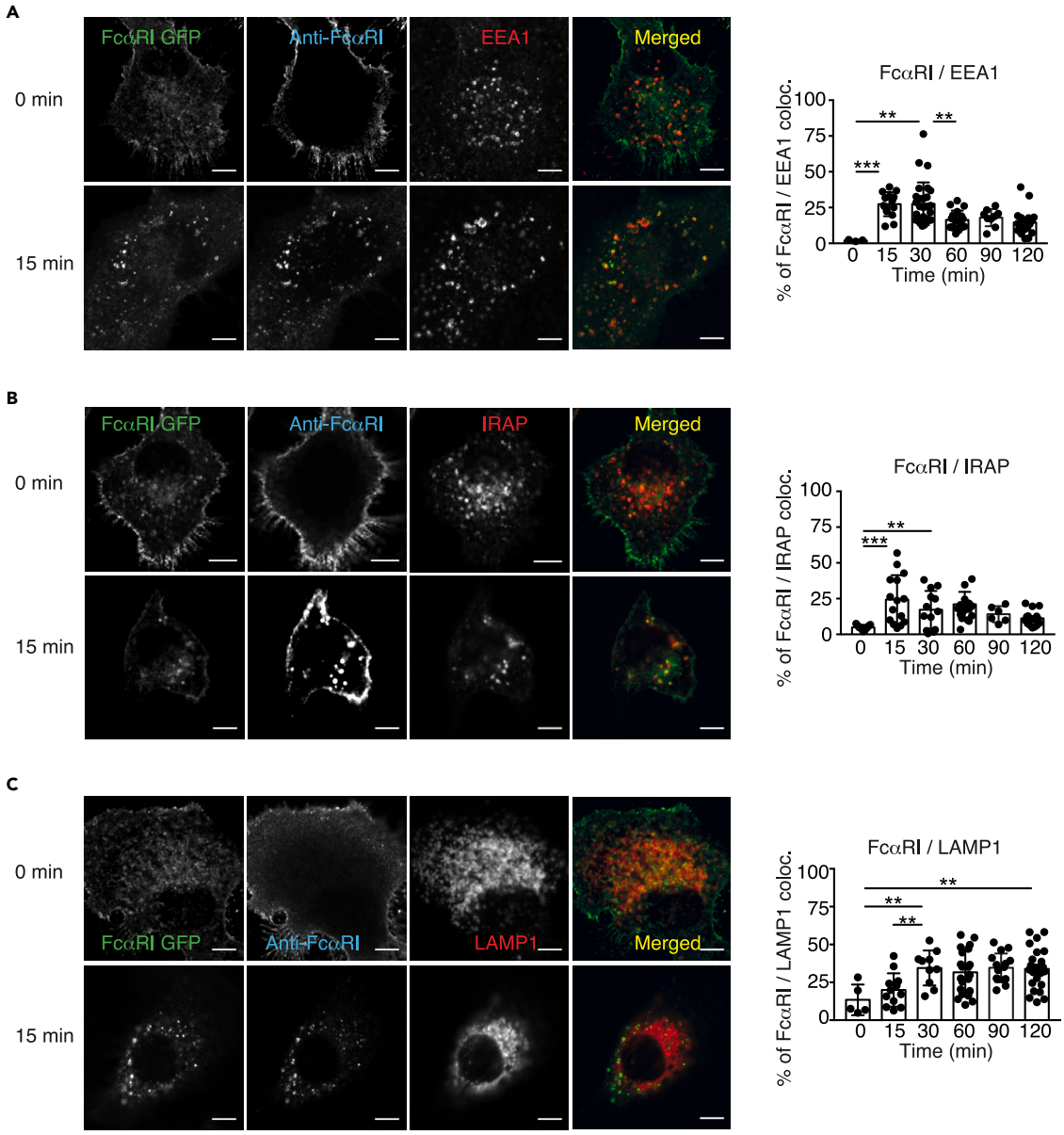

Figure 3. After cross-linking, FcαRI is targeted to lysosomes

(A–C) DC2.4 cells expressing FcαRI-GFP (green) were incubated with mouse anti-human FcαRI (clone A77) and cross-linked with anti-mouse IgG (blue) at 4°C. After removal of excess antibodies, the cells were shifted for the indicated time points at 37°C, fixed and stained for EEA1 (red) (A), IRAP (red) (B), and LAMP1 (red) (C). The pictures show representative images from three independent experiments and the graphs show colocalization between FcαRI and the endocytic markers. Each dot represents a cell. Data are represented as mean ± SEM. Scale bars = 5 μm. *p < 0.05; **p < 0.01; ***p < 0.001; ****p < 0.0001.

and co-immunoprecipitation data, suggests that IRAP storage endosomes could act as endosomal-signaling platforms for the FcγRI.

IRAP deletion affects the endosomal recruitment of signaling partners to FcγRI

Considering the previously demonstrated role of IRAP in storage endosome trafficking[14] and TLR9[3] and TCR activation,[4] we wondered if, similar to TLR9 and TCR, FcγRI trafficking or signaling was affected in the absence of IRAP. Since the DC2.4 cell line was not viable when we depleted IRAP, we used bone marrow-derived dendritic cells (BM-DCs) obtained from wild type and IRAP-deficient mice[15] to investigate trafficking of both chains of endogenous FcγRI, the alpha chain encoded by the *Fcgr1* gene and the common FcR-γ-chain associated with FcRs, encoded by the *Fcer1g* gene.[16] While in wt BM-DCs FcγRI colocalized in

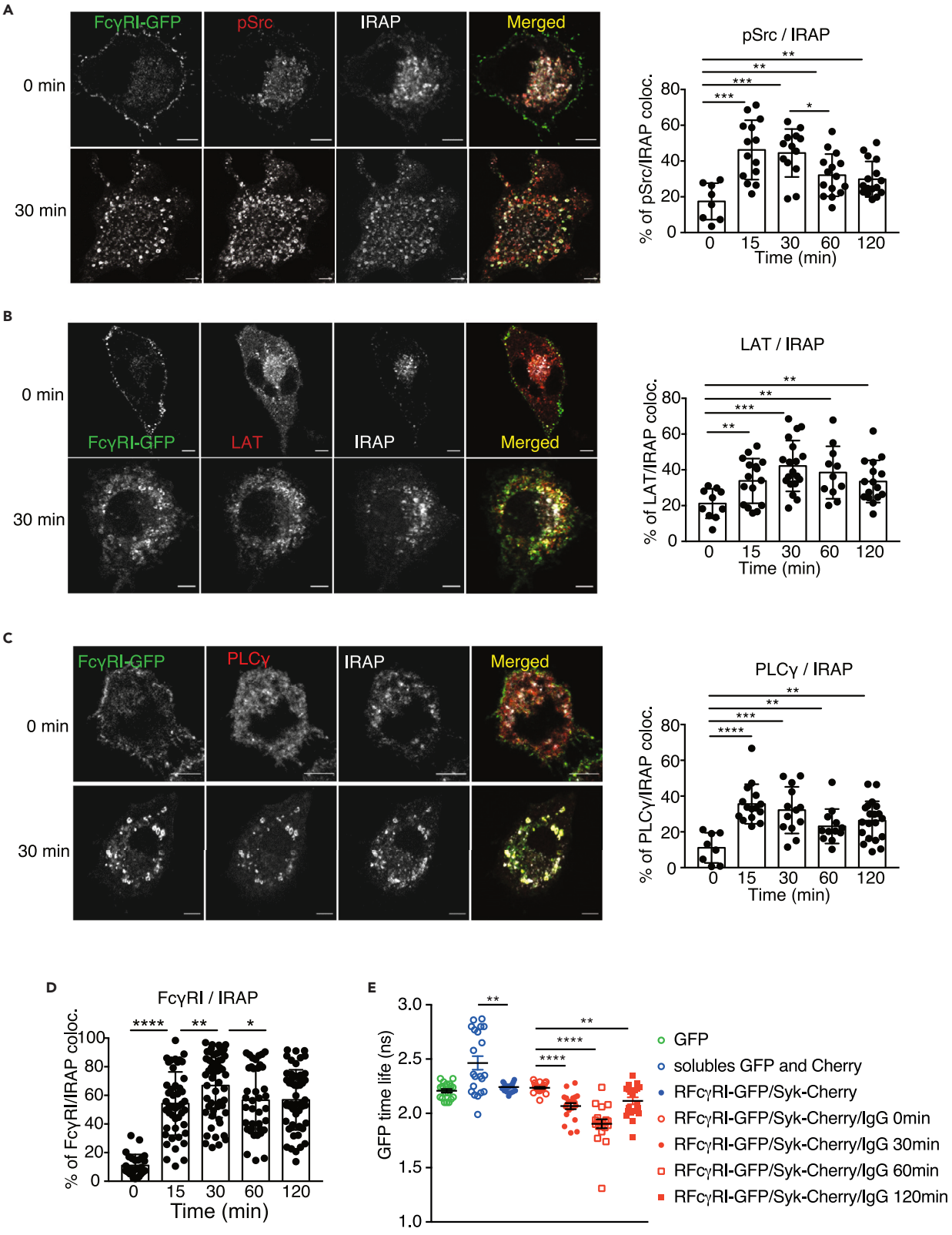
A
FcγRI-GFP
pSrc
IRAP
Merged
0 min
30 min
pSrc / IRAP
% of pSrc/IRAP coloc.
Time (min)
B
FcγRI-GFP
LAT
IRAP
Merged
0 min
30 min
LAT / IRAP
% of LAT/IRAP coloc.
Time (min)
C
FcγRI-GFP
PLCγ
IRAP
Merged
0 min
30 min
PLCγ / IRAP
% of PLCγ/IRAP coloc.
Time (min)
D
FcγRI / IRAP
% of FcγRI/IRAP coloc.
Time (min)
E
GFP time life (ns)
GFP
solubles GFP and Cherry
RFcγRI-GFP/Syk-Cherry
RFcγRI-GFP/Syk-Cherry/IgG 0min
RFcγRI-GFP/Syk-Cherry/IgG 30min
RFcγRI-GFP/Syk-Cherry/IgG 60min
RFcγRI-GFP/Syk-Cherry/IgG 120min

Figure 4. Activated FcγRI recruits signaling partners at the level of IRAP endosomes

(A–C) DC2.4 cells expressing FcγRI-GFP (green) were incubated with human IgG and anti-human IgG at 4°C. After removal of excess antibodies, cells were shifted for the indicated time points at 37°C, fixed and stained for: pSrc (red) and IRAP (gray) (A), LAT (red) and IRAP (gray) (B), or PLCγ (red) and IRAP (gray) (C). The pictures show representative images from three independent experiments and the graphs show colocalization between the indicated signalosome component and IRAP. Each dot represents a cell. Scale bars = 5 μm.

(D) The graph shows the colocalization between FcγRI and IRAP that was quantified in the conditions (A), (B) and (C).

(E) The interaction of FcγRI with Syk was measured by FLIM experiments and the graph shows the GFP lifetime for cells expressing only GFP, both GFP and mCherry as soluble proteins and the cells expressing both FcγRI-GFP and Syk-mCherry in steady state and after the receptor crosslinking for indicated time points. In all the graphs, each dot represents a cell. Data are represented as mean ± SEM. Scale bars = 5 μm.

*p < 0.05; **p < 0.01; ***p < 0.001; ****p < 0.0001.

endosomes with the FcR-γ-chain for as long as 2 h after receptor cross-linking with the anti-murine Fcgr1-specific antibody, in the absence of IRAP this colocalization was lost at 2 h and both Fcgr1 and the FcR-γ-chain showed weak to undetectable staining (Figure 5A). This suggests that in the absence of IRAP, both chains of activated FcγRI are targeted to degradation. Moreover, at early time points, when the FcR-γ-chain was still detectable in IRAP-deficient BM-DCs, we observed that colocalization between the FcR-γ-chain and active Syk (Figure 5B) was reduced in the absence of IRAP (Figure 5B). These results indicate that IRAP is required for the stabilization of endosomal signaling platforms of the endogenous murine FcγRI.

The major small GTPase recruited on IRAP$^+$ endosomes in BM-DCs is Rab14, and we have previously shown that Rab14 interacts with the kinesin KIF16B. The Rab14-KIF16B complex is involved in the anterograde transport of IRAP endosomes along microtubules and in their fusion with early endosomes and newly formed phagosomes.[17] Since Rab14 depletion destabilizes IRAP endosomes, we hypothesized that FcγRI endosomal signaling would also be affected in the absence of Rab14. To investigate this hypothesis, we depleted Rab14 in DC2.4 cells using specific lentiviral shRNA (Figure S4A) and investigated FcγRI colocalization with IRAP and active Syk. In the absence of Rab14, FcγRI colocalization with IRAP was lower than in control cells (Figure S4B), probably because the absence of Rab14 decreases the stability of IRAP$^+$ endosomes, as previously published.[17,18] In parallel with the decrease in colocalization between FcγRI and IRAP, the amount of pSyk recruited to FcγRI was significantly decreased in Rab14 depleted cells for all time points analyzed (Figure S4C). These results indicate that Rab14 is involved in the sustained endosomal signaling of FcγRI, probably by limiting the retrograde transport of endosomes toward lysosomes, as previously demonstrated.[17]

IRAP-deficient macrophages show reduced FcγRI function

Altogether, our cell biology and biochemical investigation revealed the importance of IRAP in the persistence of activated FcRs in the endosomal compartment and its potential impact on downstream signaling. To test the potential impact of IRAP deletion on FcγR function, we measured the production of pro-inflammatory cytokines by wt and IRAP-deficient BM-DCs after FcR activation. In the case of BM-DC activation by FcγR cross-linking, IRAP-deficient cells produced less pro-inflammatory cytokines than wt cells (Figure 6A). This effect was not due to a lack of ability of IRAP deficient cells to produce proinflammatory cytokines, since BM-DCs activation with LPS, led to similar levels of pro-inflammatory cytokine secretion in both wt and IRAP-deficient cells (Figure 6A), as previously published.[3]

As a second readout of FcγR signaling, we performed an ADCC assay.[19] Since in mice, the main cellular population involved in ADCC are macrophages (MFs),[20] we first verified that the cell surface expression of FcγRI (Figure S5A) and FcγRI internalization and recycling (Figure S5B) were not affected by IRAP deletion in MFs. Moreover, similar to BM-DCs, in MFs, the activated receptor was internalized in IRAP endosomes (Figure S5C) and recruited pSyk at the endosomal level (Figure S5D).

We used wt and IRAP-deficient peritoneal macrophages (MFs) as effector cells, the HUCCT1 cholangiocarcinoma cell line expressing EGFR as target cells and an anti-EGFR antibody to trigger the IgG2a-mediated cell cytotoxicity, a phenomenon in which FcγRI has a predominant role.[21] After two days of incubation of MFs with HUCCT1 cells, in the presence of increasing anti-EGFR antibody concentrations, we observed that IRAP-deficient MFs killed tumor cells less efficiently than wt MFs (Figure 6B). These results confirmed the hypothesis that IRAP is required for efficient FcR-mediated cellular response.

DISCUSSION

Our study showed that activating FcγRs use endosomal signaling platforms, similar to other immune receptors, such as the TCR[4–6] and to non-immune cell surface receptors such as RTKs.[2] These results are

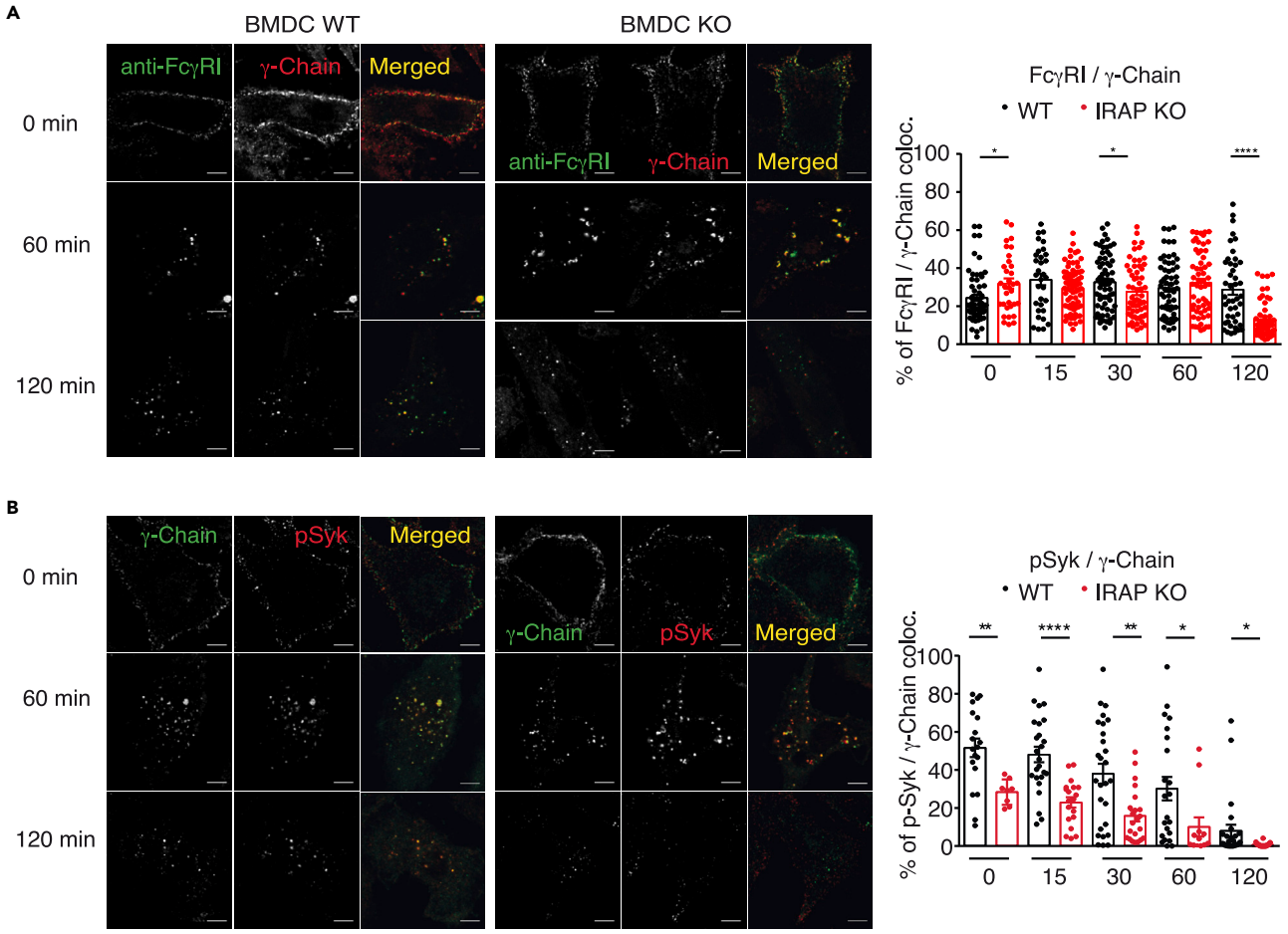

Figure 5. IRAP deletion affects the endosomal recruitment of active Syk to FcγRI

(A and B) Wild-type (WT) or IRAP-deficient (KO) BM-DCs were incubated with anti-mouse FcγRI (clone AT152-9), followed by crosslinking with non-labeled anti-rat IgG at 4°C. After removal of excess antibodies, the cells were shifted for the indicated time points at 37°C, fixed and stained for endogenous FcγRI (green) and γ-chain (red) in (A) and for γ-chain (green) and Syk phosphorylated on Tyrosine 352 (pSyk) (red) in (B). The pictures show representative images from three independent experiments and the graphs show colocalization between FcγRI and the γ-chain (A) and colocalization between the γ-chain and phosphorylated, active Syk (B). Each dot represents a cell. Data are represented as mean ± SEM. Scale bars = 5 μm. *p < 0.05; **p < 0.01; ***p < 0.001; ****p < 0.0001.

compatible with previous studies showing that activated FcγRs are massively internalized but bring crucial information about FcR trafficking, especially for the time frame of 5–60 min after receptor activation. Pioneer studies of FcγR trafficking have shown that FcγR activation by IC induces FcγR internalization and their final targeting to lysosomes.[22] However, both the study of receptor intracellular trafficking upon activation by IC[23] and the kinetics of IC degradation[22] showed that the targeting of FcγR and their ligands to lysosomal compartments occurs at late time points of activation, which exceed 60 min. These initial studies did not address the precise intracellular compartments to which FcγRs are targeted within the 60 min time window, before being degraded in lysosomes.

We decided to follow FcRs trafficking during this time window and to investigate if FcRs are able to signal from endosomal vesicles, similar to the CD3ζ chain of the TCR.[4,14] The hypothesis of FcR endosomal signaling was supported by the high-structural homology between the CD3ζ chain of the TCR and the γ-chain of FcRs, which is functionally relevant, because each protein can complement the absence of the other.[7,8]

Our results show that similar to TCR activation, the activation of FcγR by cross-linking is followed by receptor internalization in endosomal vesicles described by IRAP and Rab14. Similar to the TCR, the FcγRs were

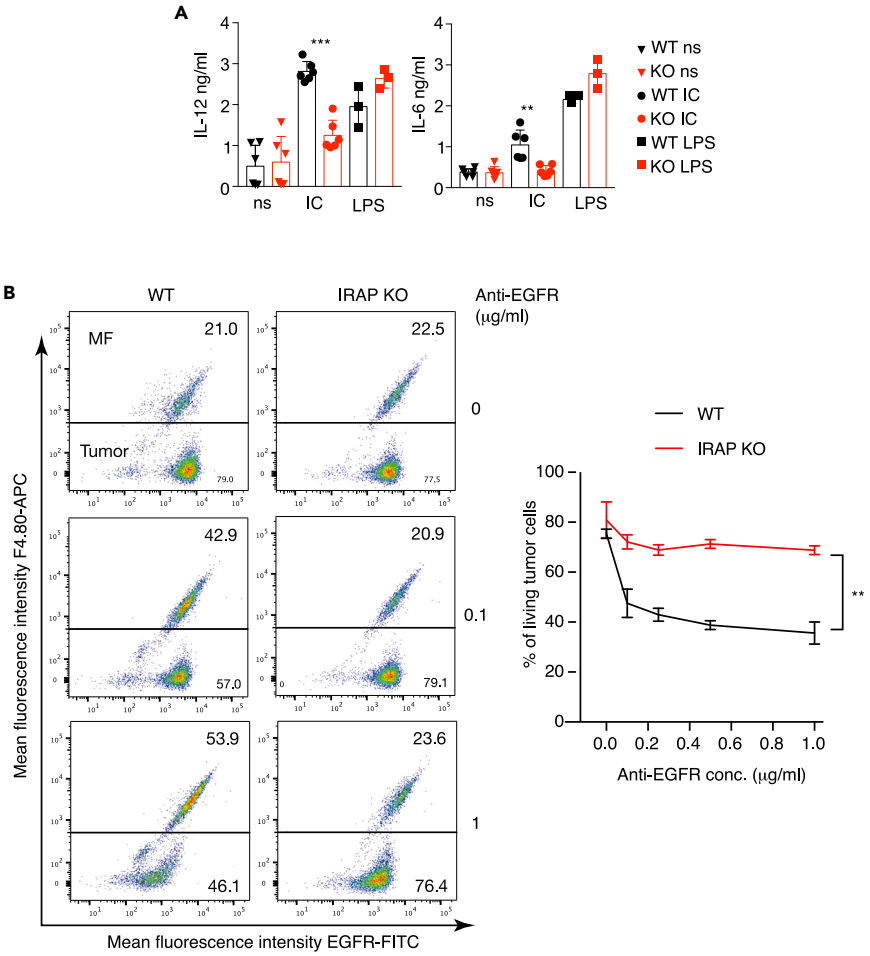

Figure 6. IRAP-deficient macrophages show reduced ADCC

(A) Wild-type (WT) or IRAP-deficient (KO) BM-DCs were activated with immune complexes (IC) or LPS and 24h later the Il-6 and IL-12 secretion was measured by ELISA (ns = nonstimulated). Each symbol represents an individual cell culture. Data are from 2 experiments.

(B) WT or IRAP-deficient peritoneal MFs were incubated with HUCCT1 tumor cells expressing EGFR in the presence of indicated concentrations of mouse IgG2a anti-EGFR antibody. After 3 days the cells were stained with anti-F4/80 to identify MFs and with mouse IgG1 anti-EGFR, followed by FITC conjugated goat F(ab')2 anti-mouse IgG1 to identify the tumor cells. The pictures show representative images from three independent experiments and the graph shows the percentage of live HUCCT1 cells defined as EGFR positive and F4/80 negative cells. Data are represented as mean ± SEM.

*p < 0.05; **p < 0.01; ***p < 0.001; ****p < 0.0001.

retained in these endosomal compartments for at least 60 min (Figures 1, 4). The association of FcγR with the components of the FcR signalosome (Figures 4, S3)) in IRAP$^+$ endosomes suggests that the receptors can use these endosomes as an intracellular signaling platform. Unlike IgG receptors included in this study, the IgA receptor FcαRI did not accumulate in IRAP$^+$ endosomes and was directly targeted to lysosomes (Figures 3, and S2). This result reflects an authentic difference between the intracellular trafficking of IgG and IgA receptors, since both the A77 antibody, which binds to EC2 of FcαRI and ICs containing IgA which bind to the EC1 domain of FcαRI[13] induced a similar rapid lysosomal targeting of the IgA receptor.

The IgG receptor endosomal signaling platforms identified in this study are localized in a particular endosome population whose stability depends on IRAP and Rab14. IRAP contributes to endosomal stability by interacting with actin cytoskeleton and the retromer,[11,14,24] while Rab14 interacts with the anterograde motor KIF16B and transports the endosomes to the cell periphery, limiting their fusion with the lysosomes.[17] Considering the role of IRAP and Rab14 in the trafficking of the endosomes containing activating FcγRs, it is

expected that in the absence of Rab14 or IRAP, the receptors will be transported to lysosomes and degraded. This hypothesis is supported by the observation that FcγR1 staining was lost in the absence of IRAP (Figure 5). Similar mechanisms were demonstrated for EGFR in HeLa cells, where Rab14-KIF16B activity prevents EGFR targeting to lysosomes, thus facilitating receptor recycling and signaling.[25]

Our study analyzed the functional impact of FcγR endosomal signaling by measuring the production of IL-12 and IL-6 and ADCC efficiency in wt and IRAP-deficient BM-DCs and MFs, respectively. These *in vitro* functional results (Figure 6) could be complemented by *in vivo* experiments using mouse models of FcγR-mediated inflammation or ADCC-based immunotherapies. Such experiments were recently performed by our collaborators and showed that mice with constitutive deletion of IRAP are resistant to anaphylaxis and collagen-induced arthritis.[26] These experiments strongly suggest that IRAP-dependent endosomal signaling is relevant for FcγR-mediated diseases. Nevertheless, the development of new mouse strains with a targeted deletion of Rab14 or IRAP exclusively in myeloid cells is required to fully demonstrate *in vivo* the role of endosomal immunoglobulin receptor signaling in the physiopathology of IC-mediated diseases. This is mandatory for Rab14, since constitutive Rab14 deletion is lethal[27] and very important for IRAP, since IRAP has a broad expression in the immune system, where it regulates several processes.[14]

The results of this work describe a previously unknown aspect of the regulatory function of IRAP in immune cells. IRAP is a type II transmembrane protein.[11] In the immune system, its carboxy-terminal enzymatic activity is involved in antigen processing,[28,29] while the cytosolic amino-terminal domain, rich in endocytic trafficking motifs limits TLR9 activation,[3] facilitates TCR signaling[4] and according to the present results, facilitates FcγR signaling. Further studies, such as identification of protein interaction of IRAP in both myeloid cells and lymphocytes are required to identify other potential cargos of IRAP endosomes and characterize the signaling pathways that are triggered at the level of IRAP endosomes. Such experiments remain very challenging, because our attempts to purify the protein complexes associated with IRAP, via tandem affinity purification were not successful. We suppose that the multiple interactions between the IRAP cytosolic tail and the cytoskeleton components[14] led to the inaccessibility of the tags in the absence of strong detergents. An alternative strategy could be a protein labeling assay[30] to decipher the IRAP interactome *in situ* and to better understand its regulatory role in immune receptors trafficking and signaling.

Limitations of the study

While our study indicates that, similar to the TCR, activating FcγRs can use IRAP-dependent endocytic signaling platforms, it has some limitations. Thus, it is solely based on data obtained *in vitro*, using the DC2.4 cell line and primary cells, such as BM-DCs and peritoneal MFs. These *in vitro* experiments showed that, in the absence of IRAP and Rab14, FcγR-mediated cytokine secretion and ADCC are compromised. Additional work will be required to identify the molecular mechanisms by which IRAP and Rab14 stabilize the endocytic signaling of FcγRs and to validate that IRAP deletion leads to the degradation of internalized receptors. In addition, the *in vivo* impact of IRAP and Rab14 on FcγR-mediated inflammatory response and ADCC should be addressed using mice with conditional IRAP or Rab14 deletion in the myeloid compartment.

STAR★METHODS

Detailed methods are provided in the online version of this paper and include the following:

- KEY RESOURCES TABLE
- RESOURCE AVAILABILITY
  - Lead contact
  - Materials availability
  - Data and code availability
- EXPERIMENTAL MODEL AND STUDY PARTICIPANT DETAILS
  - Mice
  - Cell culture
  - Plasmid constructs and cell transfection
  - Antibodies
  - Lentivirus production and transduction
  - Receptor aggregation for the microscopy assays

- Immunofluorescence microscopy
- Receptor aggregation for the biochemical assays (WB, Co-IP)
- Co-immunoprecipitation and immunoblots
- FLIM (Fluorescence Lifetime imaging microscopy)
- ELISA
- ADCC
- FcR internalization and IC recycling

- QUANTIFICATION AND STATISTICAL ANALYSIS

SUPPLEMENTAL INFORMATION

Supplemental information can be found online at https://doi.org/10.1016/j.isci.2023.107055.

ACKNOWLEDGMENTS

We thank the Labex Inflamex and the Agence Nationale de la Recherche (ANR grants Cytoendostor, ECLIPSE and Help2Kill) and FRM (fellowship to DK) for financial support. We thank A. Couvineau (Inserm U1149, Paris) for providing the HUCCT1 cell line. We also thank Meriem Garfa-Traore of the Imaging Core Facility of SFR Necker for helping with FLIM-FRET analysis and Gregory Gauthier for his help with peritoneal macrophage isolation.

AUTHOR CONTRIBUTIONS

Conceptualization: L.S and S.B; Methodology: Most experiments were performed by S.B, with help from M.N, D. K., and M.B, I.E and R.M helped with advice on experiments and contributed to critical reading of the manuscript, M.C. D. L. performed a part of molecular cloning; Writing - original draft: L.S and S.B., revised version- I.E and L.S; Funding acquisition: L.S.

DECLARATION OF INTERESTS

The authors declare that they have no conflict of interest.

Received: October 12, 2022
Revised: April 2, 2023
Accepted: June 1, 2023
Published: June 9, 2023

REFERENCES

1. Di Guglielmo, G.M., Baass, P.C., Ou, W.J., Posner, B.I., and Bergeron, J.J. (1994). Compartmentalization of SHC, GRB2 and mSOS, and hyperphosphorylation of Raf-1 by EGF but not insulin in liver parenchyma. EMBO J. *13*, 4269–4277.

2. Bergeron, J.J.M., Di Guglielmo, G.M., Dahan, S., Dominguez, M., and Posner, B.I. (2016). Spatial and temporal regulation of receptor tyrosine kinase activation and intracellular signal transduction. Annu. Rev. Biochem. *85*, 573–597. https://doi.org/10.1146/annurev-biochem-060815-014659.

3. Babdor, J., Descamps, D., Adiko, A.C., Tohmé, M., Maschalidi, S., Evnouchidou, I., Vasconcellos, L.R., De Luca, M., Mauvais, F.-X., Garfa-Traore, M., et al. (2017). IRAP+ endosomes restrict TLR9 activation and signaling. Nat. Immunol. *18*, 509–518. https://doi.org/10.1038/ni.3711.

4. Evnouchidou, I., Chappert, P., Benadda, S., Zucchetti, A., Weimershaus, M., Bens, M., Caillens, V., Koumantou, D., Lotersztajn, S., van Endert, P., et al. (2020). IRAP-dependent endosomal T cell receptor signalling is essential for T cell responses. Nat. Commun. *11*, 2779. https://doi.org/10.1038/s41467-020-16471-7.

5. Yudushkin, I.A., and Vale, R.D. (2010). Imaging T-cell receptor activation reveals accumulation of tyrosine-phosphorylated CD3ζ in the endosomal compartment. Proc. Natl. Acad. Sci. USA *107*, 22128–22133. https://doi.org/10.1073/pnas.1016388108.

6. Willinger, T., Staron, M., Ferguson, S.M., De Camilli, P., and Flavell, R.A. (2015). Dynamin 2-dependent endocytosis sustains T-cell receptor signaling and drives metabolic reprogramming in T lymphocytes. Proc. Natl. Acad. Sci. USA *112*, 4423–4428. https://doi.org/10.1073/pnas.1504279112.

7. Rodewald, H.R., Arulanandam, A.R., Koyasu, S., and Reinherz, E.L. (1991). The high affinity Fc epsilon receptor gamma subunit (Fc epsilon RI gamma) facilitates T cell receptor expression and antigen/major histocompatibility complex-driven signaling in the absence of CD3 zeta and CD3 eta. J. Biol. Chem. *266*, 15974–15978.

8. Howard, F.D., Rodewald, H.R., Kinet, J.P., and Reinherz, E.L. (1990). CD3 zeta subunit can substitute for the gamma subunit of Fc epsilon receptor type I in assembly and functional expression of the high-affinity IgE receptor: evidence for interreceptor complementation. Proc. Natl. Acad. Sci. USA *87*, 7015–7019. https://doi.org/10.1073/pnas.87.18.7015.

9. Mócsai, A., Ruland, J., and Tybulewicz, V.L.J. (2010). The SYK tyrosine kinase: a crucial player in diverse biological functions. Nat. Rev. Immunol. *10*, 387–402. https://doi.org/10.1038/nri2765.

10. Getahun, A., and Cambier, J.C. (2015). Of ITIMs, ITAMs, and ITAMis: revisiting immunoglobulin Fc receptor signaling. Immunol. Rev. *268*, 66–73. https://doi.org/10.1111/imr.12336.

11. Saveanu, L., and van Endert, P. (2012). The role of insulin-regulated aminopeptidase in MHC class I antigen presentation. Front. Immunol. *3*, 57. https://doi.org/10.3389/fimmu.2012.00057.

12. Monteiro, R.C., Cooper, M.D., and Kubagawa, H. (1992). Molecular heterogeneity of Fc alpha receptors detected

by receptor-specific monoclonal antibodies. J. Immunol. *148*, 1764–1770.

13. Morton, H.C., van Zandbergen, G., van Kooten, C., Howard, C.J., van de Winkel, J.G., and Brandtzaeg, P. (1999). Immunoglobulin-binding sites of human FcalphaRI (CD89) and bovine Fcgamma2R are located in their membrane-distal extracellular domains. J. Exp. Med. *189*, 1715–1722. https://doi.org/10.1084/jem.189.11.1715.

14. Descamps, D., Evnouchidou, I., Caillens, V., Drajac, C., Riffault, S., van Endert, P., and Saveanu, L. (2020). The role of insulin regulated aminopeptidase in endocytic trafficking and receptor signaling in immune cells. Front. Mol. Biosci. *7*, 583556. https://doi.org/10.3389/fmolb.2020.583556.

15. Keller, S.R., Davis, A.C., and Clairmont, K.B. (2002). Mice deficient in the insulin-regulated membrane aminopeptidase show substantial decreases in glucose transporter GLUT4 levels but maintain normal glucose homeostasis. J. Biol. Chem. *277*, 17677–17686. https://doi.org/10.1074/jbc.M202037200.

16. Brandsma, A.M., Hogarth, P.M., Nimmerjahn, F., and Leusen, J.H.W. (2016). Clarifying the confusion between cytokine and Fc receptor "common gamma chain. Immunity *45*, 225–226. https://doi.org/10.1016/j.immuni.2016.07.006.

17. Weimershaus, M., Mauvais, F.-X., Saveanu, L., Adiko, C., Babdor, J., Abramova, A., Montealegre, S., Lawand, M., Evnouchidou, I., Huber, K.J., et al. (2018). Innate immune signals induce anterograde endosome transport promoting MHC class I cross-presentation. Cell Rep. *24*, 3568–3581. https://doi.org/10.1016/j.celrep.2018.08.041.

18. Weimershaus, M., Mauvais, F.-X., Evnouchidou, I., Lawand, M., Saveanu, L., and van Endert, P. (2020). IRAP endosomes control phagosomal maturation in dendritic cells. Front. Cell Dev. Biol. *8*, 585713. https://doi.org/10.3389/fcell.2020.585713.

19. de Haij, S., Jansen, J.H.M., Boross, P., Beurskens, F.J., Bakema, J.E., Bos, D.L., Martens, A., Verbeek, J.S., Parren, P.W.H., van de Winkel, J.G.J., and Leusen, J.H.W. (2010). In vivo cytotoxicity of type I CD20 antibodies critically depends on Fc receptor ITAM signaling. Cancer Res. *70*, 3209–3217. https://doi.org/10.1158/0008-5472.CAN-09-4109.

20. Uchida, J., Hamaguchi, Y., Oliver, J.A., Ravetch, J.V., Poe, J.C., Haas, K.M., and Tedder, T.F. (2004). The innate mononuclear phagocyte network depletes B lymphocytes through Fc receptor-dependent mechanisms during anti-CD20 antibody immunotherapy. J. Exp. Med. *199*, 1659–1669. https://doi.org/10.1084/jem.20040119.

21. Ioan-Facsinay, A., de Kimpe, S.J., Hellwig, S.M.M., van Lent, P.L., Hofhuis, F.M.A., van Ojik, H.H., Sedlik, C., da Silveira, S.A., Gerber, J., de Jong, Y.F., et al. (2002). FcgammaRI (CD64) contributes substantially to severity of arthritis, hypersensitivity responses, and protection from bacterial infection. Immunity *16*, 391–402.

22. Bonnerot, C., Briken, V., Brachet, V., Lankar, D., Cassard, S., Jabri, B., and Amigorena, S. (1998). Syk protein tyrosine kinase regulates Fc receptor gamma-chain-mediated transport to lysosomes. EMBO J. *17*, 4606–4616. https://doi.org/10.1093/emboj/17.16.4606.

23. Zhang, C.Y., and Booth, J.W. (2010). Divergent intracellular sorting of FcγRIIA and FcγRIIB2. J. Biol. Chem. *285*, 34250–34258. https://doi.org/10.1074/jbc.M110.143834.

24. Pan, X., Meriin, A., Huang, G., and Kandror, K.V. (2019). Insulin-responsive amino peptidase follows the Glut4 pathway but is dispensable for the formation and translocation of insulin-responsive vesicles. Mol. Biol. Cell *30*, 1536–1543. https://doi.org/10.1091/mbc.E18-12-0792.

25. Hoepfner, S., Severin, F., Cabezas, A., Habermann, B., Runge, A., Gillooly, D., Stenmark, H., and Zerial, M. (2005). Modulation of receptor recycling and degradation by the endosomal kinesin KIF16B. Cell *121*, 437–450. https://doi.org/10.1016/j.cell.2005.02.017.

26. Bratti, M., Vibhushan, S., Longé, C., Koumantou, D., Ménasché, G., Benhamou, M., Varin-Blank, N., Blank, U., Saveanu, L., and Ben Mkaddem, S. (2022). Insulin-regulated aminopeptidase contributes to setting the intensity of FcR-mediated inflammation. Front. Immunol. *13*, 1029759. https://doi.org/10.3389/fimmu.2022.1029759.

27. Ueno, H., Huang, X., Tanaka, Y., and Hirokawa, N. (2011). KIF16B/Rab14 molecular motor complex is critical for early embryonic development by transporting FGF receptor. Dev. Cell *20*, 60–71. https://doi.org/10.1016/j.devcel.2010.11.008.

28. Saveanu, L., Carroll, O., Weimershaus, M., Guermonprez, P., Firat, E., Lindo, V., Greer, F., Davoust, J., Kratzer, R., Keller, S.R., et al. (2009). IRAP identifies an endosomal compartment required for MHC class I cross-presentation. Science *325*, 213–217. https://doi.org/10.1126/science.1172845.

29. Segura, E., Albiston, A.L., Wicks, I.P., Chai, S.Y., and Villadangos, J.A. (2009). Different cross-presentation pathways in steady-state and inflammatory dendritic cells. Proc. Natl. Acad. Sci. USA *106*, 20377–20381. https://doi.org/10.1073/pnas.0910295106.

30. Dionne, U., and Gingras, A.-C. (2022). Proximity-dependent biotinylation approaches to explore the dynamic compartmentalized proteome. Front. Mol. Biosci. *9*, 852911. https://doi.org/10.3389/fmolb.2022.852911.

31. Manders, E.M.M., Verbeek, F.J., and Aten, J.A. (1993). Measurement of co-localization of objects in dual-colour confocal images. J. Microsc. *169*, 375–382. https://doi.org/10.1111/j.1365-2818.1993.tb03313.x.

STAR★METHODS

KEY RESOURCES TABLE

REAGENT or RESOURCE	SOURCE	IDENTIFIER
Antibodies		
Anti-human FcγRI	BioRad	Cat# MCA756PET; RRID: AB_1102275
Anti-IRAP	Cell Signaling	Cat# 6918; RRID: AB_10860248 Cat# 9876; RRID: AB_10897856
Anti-TGN38	Thermo Fisher Scientific	Cat# PA1-33044; RRID: AB_2203275
Anti-LAMP1	Thermo Fisher Scientific	Cat# 13-1071-82; RRID: AB_657544
Anti-EEA1 goat polyclonal	Santa Cruz	N-19, Discontinued
Anti-Syk	Cell Signaling	Cat# 13198; RRID: AB_2687924
Anti-phospho-Syk-tyr352	Cell Signaling	Cat# 73382; RRID: AB_2799838
Anti-PLCγ	Santa Cruz	Cat# sc-7290; RRID: AB_628119
Anti-LAT	Millipore	Cat# 06-807; RRID: AB_310252
Anti-pSrc	Cell Signaling	Cat# 6943; RRID: AB_10013641
Anti-γ chain	MBL	Clone 1D6, Cat# M-191-3
Donkey anti-rabbit A647	Invitrogen	Cat# A-31573; RRID: AB_2536183
Donkey anti-rabbit A405	Abcam	Cat# ab150075; RRID: AB_2752244
Donkey anti-goat A405	Abcam	Cat# ab175651; RRID: AB_2923541
Donkey anti-rat A405	Abcam	Cat# ab175664; RRID: AB_2313502
Donkey anti-mouse A594	Invitrogen	Cat# A-21203; RRID: AB_141633
Donkey anti-mouse A647	Invitrogen	Cat# A-31571; RRID: AB_162542
Donkey anti-mouse A488	Invitrogen	Cat# A-21202; RRID: AB_141607
Goat anti-donkey DyeLight 650	Invitrogen	Cat# SA5-10089; RRID: AB_2556669
Anti-mouse FcγRI	BioRad	Cat# MCA5997; RRID: AB_2687456
Anti-human FcγRIIA	Stemcell Technologies	Cat# 60012FI; RRID: AB_2722545
Anti-human FcαRI	Produced in R. Monteiro Lab.	Clone A77
Anti-Rab14	Sigma Aldrich	Cat# R0656; RRID: AB_1841128
Human polyclonal IgG, ChromPure	Jackson ImmunoResearch	Cat# 009-000-003; RRID: AB_2337043
Donkey anti-human IgG	Jackson ImmunoResearch	Cat# 709-005-149; RRID: AB_2340483
Donkey anti-rat	Jackson ImmunoResearch	Cat# 712-005-153; RRID: AB_2340631
Human IgA	Bethyl Laboratories	Cat# P80-102; RRID: AB_2892036
Goat anti-human IgA	Sigma Aldrich	Cat# I0884; RRID: AB_260111
Anti-EGFR	Invitrogen	Cat# MA5-12875; RRID: AB_10978829
F4/80 APC	BioLegend	Cat# 123116; RRID: AB_893481
Anti-EGFR	ThemoFisher Scientific	Cat# MA5-12880; RRID: AB_10982150
Goat F(ab')2 anti-mouse IgG1	Southern Biotech	Cat# 1072-09; RRID: AB_2794434
Anti-mouse FcγRI PE	Invitrogen	Cat# 12-0641-82; RRID: AB_2735014
Anti-GFP for western blot	Sigma Aldrich	Cat# 11814460001; RRID: AB_390913
Bacterial strains		
E. Coli One Shot™ Stbl3™	ThermoFisher Scientific	Cat. #C737303
Chemicals, peptides, and recombinant proteins		
GM-CSF	Peprotech	Cat. # 315-03
IMDM	Gibco	Cat. # 11504556
RPMI	Gibco	Cat. # 31966

(*Continued on next page*)

Continued

REAGENT or RESOURCE	SOURCE	IDENTIFIER
DMEM	Gibco	Cat. # 72400
Glutamine	Gibco	Cat. # 11539876
Peni-Strepto	Gibco	Cat. # 15140122
b-mercaptoethanol	Gibco	Cat. # 31350010
Fetal calf serum lot 2357916	Gibco	Cat. #10270-106
ACK Lysis Buffer	Gibco	Cat. # 10492
BES	Sigma Aldrich	Cat. #B9879
$CaCl_2$	Sigma Aldrich	Cat. #C5670
NaCl	Sigma Aldrich	Cat. #S9625
Na_2HPO_4	Sigma Aldrich	Cat. # RDD038
Puromycin	Sigma Aldrich	Cat. #P8833
Polybrene	Sigma Aldrich	Cat. # 107689
Bovine Fibronectin	ThermoFisher Scientific	Cat. # 33010018
Protease inhibitors	Sigma Aldrich	Cat. # 11873580001
Phosphatase inhibitors cocktails 1 and 2	Sigma Aldrich	P2850 and P5726
LPS	Invivogen	LPS-B5
Sodium Thioglycolate	Conalab	Cat. # 1508.00
Critical commercial assays		
GFP-trap beads	Chromotek	Cat. # gta-20
Criterion 4–15% acrylamide gels	BioRad	Cat. # 5671084
PVDF membranes	BioRad	Cat. # 17001919
Clarity™ Western ECL Substrate	BioRad	Cat. # 1705061
Macrophage Isolation Kit	Miltenyi Biotech	Cat. # 130-110-435
IL-6 ELISA	BioLegend	Cat. # 431304
IL-12 ELISA	BioLegend	Cat. # 431603
Experimental models: Cell lines		
HUCCT1	Provided by Alain Couvineau	RRID:CVCL_0324
HEK 293 FT	ThermoFisher Scientific	Cat. #R70007
DC2.4	Sigma Aldrich	Cat. # SCC142
Experimental models: Organisms/strains		
IRAP ko mice	Provided by Susanna Keller	Published in 2002.[15]
Oligonucleotides		
FcγRI TACTCGAGATGTGGTTCTTGACAACTCT	Eurofins	Cloning oligos
FcγRI ATGGGCCCCCGTGGCCCCCTGGGGCTC	Eurofins	Cloning oligos
RFcαI TAgaattcATGGACCCCAAACAGACCac	Eurofins	Cloning oligos
RFcαI TAgcggccgcTTACTTGTACAGCTCATCCATTCC	Eurofins	Cloning oligos
Recombinant DNA		
Human FcγRI cDNA	Origene	NM_000566
sh RNA anti-Rab14	Sigma Aldrich	TRCN0000089375
pLVX-CMV-IRES-puro	Takara Bio	Cat. # 632183
pCMVDelta8.2	Addgene	Cat. #12263
pMD2G	Addgene	Cat. # 12259
pMSCV-mCherry-Syk	Addgene	Cat. # 50045
pCL-Ampho	Novusbio	Cat. # NBP2-29541

(*Continued on next page*)

Continued

REAGENT or RESOURCE	SOURCE	IDENTIFIER
Software and algorithms		
FlowJo 10	BD Biosciences	https://www.flowjo.com/
GraphPad Prism 7	GraphPad	https://www.graphpad.com/scientific-software/prism
ImageLab 4	BioRad	https://www.bio-rad.com/fr-fr/product/image-lab-software
ImageJ 2.0.0	NIH	https://imagej.nih.gov/ij/download.html
Symphotime 64	PicoQuant	https://www.picoquant.com
Affinity Designer 2	Serif	https://affinity.serif.com/fr/designer/

RESOURCE AVAILABILITY

Lead contact

Further information and requests for resources and reagents should be directed to and will be fulfilled by the lead contact, Loredana Saveanu (loredana.saveanu@inserm.fr).

Materials availability

All unique reagents generated in this study are available from the lead contact with completed materials transfer agreement.

Data and code availability

- Data reported in this paper can be shared by the lead contact upon request.
- This work does not include any original code.
- Any additional information required to reanalyze the data reported in this paper is available from the lead contact upon request.

EXPERIMENTAL MODEL AND STUDY PARTICIPANT DETAILS

Mice

Previously described IRAP deficient mice[15] were bred in our animal facility in pathogen free conditions. All animal care and experimental procedures were performed in accordance with the guidelines and regulations of the French Veterinary Department and approved by the "Comité d'Ethique pour l'Experimentation Animale" of our institute. Both male and female animals were used between 6 and 12 weeks of age and were matched for sex and age.

Cell culture

BM-DCs were produced *in vitro* by culturing bone marrow precursor cells from large bones for 7 days in complete medium (IMDM complemented with 10% FCS, 2 mM glutamine, 100 U/mL penicillin, 100 μg/mL streptomycin, 50 μM β-mercaptoethanol) supplemented with 20 μg/mL GM-CSF). DC2.4 were cultured in complete medium (IMDM complemented with 10% FCS, 2 mM glutamine, 100 U/mL penicillin, 100 μg/mL streptomycin, 50 μM β-mercaptoethanol). All the experiments were performed in the presence of 10% FCS. Peritoneal MFs were cultured in complete medium (RPMI complemented with 10% FCS, 2 mM glutamine, 100 U/mL penicillin, 100 μg/mL streptomycin). HuCCT1 and HEK293T were kept in DMEM-Glutamax complete medium.

Plasmid constructs and cell transfection

The cDNA for the different FcRs was cloned in fusion with EGFP in the pLVX-CMV-IRES-Puro plasmid (Clontech). The cDNA coding for FcγRI was amplified from the NM_000566 cDNA (Origene) with the following primers: forward 5′-TACTCGAGATGTGGTTCTTGACAACTCT-3′ (contains the XhoI restriction site) and reverse 5′-ATGGGCCCCCGTGGCCCCCTGGGGCTC-3′ (contains the ApaI restriction site), cloned into the pCRBlunt shuttle vector (Invitrogen), sequenced and transferred into pEGFP-N1 using the XhoI and ApaI restriction enzymes. Finally, the FcγRI-GFP fusion cDNA was removed from the pEGFP-N1 vector

with NheI (blunted with Klenow) and NotI and inserted into pLVX-CMV-IRES-Puro between EcoRI (blunted with Klenow) and NotI.

The cDNA coding for FcγRIIA-GFP in pLCPX vector was a kind gift from Peter Cresswell. FcγRIIA-GFP was removed from pLPCX with BglII (blunted with Klenow) and NotI and cloned into pLVX-CMV-IRES-Puro between EcoRI (blunted with Klenow) and NotI.

The FcαRI-GFP in pSelect and the cDNA coding for FcγRIIB were provided by Erwan Boedec (INSERM U1149, Paris). The RFcαI-GFP fusion cDNA was amplified with the following primers: forward 5′-TAgaattcATGGACC CCAAACAGACCac-3′ (contains the EcoRI restriction site) and reverse 5-TAgcggccgcTTACTTGTACAGCTC ATCCATTCC-3′ (contains the NotI restriction site). The PCR product was cloned into pCRBlunt (Invitrogen). After sequencing, the cDNA coding for FcαRI-GFP fusion was transferred into pLVX-CMV-IRES-Puro between EcoRI and NotI.

Antibodies

Primary antibodies used were: anti-human-FcγRI mouse monoclonal antibody (BioRad, clone 10.1), anti-IRAP rabbit monoclonal antibody (Cell Signaling, clone D7C5), anti-TGN38 rabbit polyclonal antibody (Thermo Fisher Scientific), anti-LAMP1 rat monoclonal antibody (Thermo Fisher Scientific, clone 1D4B), anti-EEA1 goat polyclonal antibody (Santa Cruz, N-19), anti-Syk rabbit monoclonal antibody (Cell Signaling clone D3ZE1), anti-phospho-Syk-Tyr352 (Cell Signaling, clone 65E4), rabbit anti-PLCγ (Santa Cruz clone E−12), rabbit anti-LAT (Millipore, clone 06–807), rabbit anti-pSrc family (Cell Signaling, clone D49G4), anti-γ chain mouse monoclonal antibody (MBL, clone 1D6) and anti-Rab14 rabbit polyclonal serum (Sigma).

Secondary antibodies used were: Alexa Fluor 647 conjugated donkey anti-rabbit (Invitrogen), Alexa Fluor 405 conjugated donkey anti-rabbit, donkey anti-rat or donkey anti-goat (Abcam) and AlexaFluor-594- or AlexaFluor-647-conjugated donkey anti-mouse (Invitrogen).

Lentivirus production and transduction

Viruses were produced by standard protocols, using the TRC consortium shRNA in pLKO.1 plasmids (www.broadinstitute.org) and the packaging plasmids pCMVDelta8.2 (Addgene #12263) and pMD2G (Addgene #12259). Briefly, 10^7 HEK-293-FT cells (Invitrogen), at 80% confluence, were transfected with the plasmid mix using CaPO4 precipitation method. The transfection mix contained 22,5 μg of pLK0.1 or pVLX plasmid, 14,7 μg pCMVDelta8.2 plasmid and 7.9 μg pMD2G plasmid in 2.5 mL of transfection buffer (0,125M $CaCl_2$, 25mM BES, 140mM NaCl, 0.75mM Na_2HPO_4). Lentiviral supernatant was collected at 24, 48 and 72 h, concentrated at 100 μL by ultracentrifugation and stored at −80°C. Then, DC2.4 or BM-DC cells were seeded in 96-well flat-bottom plates at 2×10^4 cells per well and transduced with 1 μL of concentrated lentiviral particles in the presence of 10 μg/mL polybrene. Following 90 min centrifugation at 37°C and 950×g, the lentiviral mix was replaced with complete IMDM medium. The day after, puromycin was added to the cells at 5 μg/mL and selected cells were used 4–5 days post transduction.

Receptor aggregation for the microscopy assays

DC2.4 cells, BM-DCs or peritoneal MF were seeded on fibronectin-coated slides for 16 h. To aggregate specific Fcγ receptors, cells were incubated with specific monoclonal antibodies for 15 min on ice. To aggregate FcγRI, cells were incubated with 5 μg/mL of mouse anti-human CD64, clone 10.1 (BioRad). To aggregate mouse FcγRI on BM-DCs and peritoneal MF, cells were incubated with 15 μg/mL of rat anti-mouse CD64, clone AT152-9 (BioRad). To aggregate FcγRIIA, cells were incubated with 10 μg/mL of mouse anti-human FcγRIIA, clone IV.3 (Stemcell). To aggregate FcαRI, cells were incubated with 10 μg/mL of F(ab)′2 fragment of the monoclonal mouse antibody A77. After removal of excess antibody by two washes in PBS, the receptors were cross-linked by the addition of anti-mouse or anti-rat IgG Alexa Fluor (Invitrogen) during 15 min on ice.

For experiments using IgGs to aggregate the receptors, cells were incubated for 15 min on ice with 5 μg/mL human polyclonal IgG (ChromPure, Jackson ImmunoResearch) or human IgA (Bethyl). Unbound IgGs were removed by two washes in cold PBS. The cells were then incubated with 10 μg/mL of donkey anti-human IgG (Jackson ImmunoResearch) or goat anti-human IgA (Sigma) on ice for 15 min, to aggregate the receptors. Cells were then shifted to 37°C for the time points indicated in the assays. All the incubations at 37°C were performed in complete medium, with 10% FCS.

Immunofluorescence microscopy

For all experiments cells were fixed with 2% PFA for 15 min at 37°C, permeabilized with 0.2% saponin in PBS containing 0.2% BSA and stained in the same buffer. Images were acquired on a Leica SP8 confocal microscope. Image treatment and analysis were performed with ImageJ software. Colocalization between two fluorescent markers was measured as Mander's coefficients (i.e, the proportions of each fluorescence with another) using the JACop plugin in ImageJ.[31] Colocalization was analyzed in individual cells, using only non-saturated images. On the colocalization graphs, each dot represents a cell.

Receptor aggregation for the biochemical assays (WB, Co-IP)

Cells were incubated for 15 min on ice with 5 μg/mL human polyclonal IgG (ChromPure, Jackson ImmunoResearch) and the excess of unbound IgGs was removed by two washes in PBS. The receptors were then aggregated by addition of 10 μg/mL of donkey anti-human IgG (Jackson ImmunoResearch) for 15 min on ice. The excess of unbound antibodies was removed by two washes in PBS and the cells were shifted to 37°C for the different time points of the assays.

Co-immunoprecipitation and immunoblots

Cell pellets were lysed in 50mM Tris, 150mM NaCl, 1% CHAPS supplemented with Complete protease inhibitor mix (Roche) and phosphatase inhibitor cocktails 2 and 3 (Sigma-Aldrich). Lysates were cleared by 10 min centrifugation at 15000xg and incubated with GFP-trap beads (Chromotek). The material bound on the beads was eluted in Laemmli buffer and the proteins were separated by SDS-PAGE using Criterion 4–15% acrylamide gels (BioRad) in Tris-Glycine-SDS buffer. The proteins were transferred on PVDF membranes (BioRad) using a Trans-Blot Turbo Transfer System from BioRad. Membranes were blocked overnight in 4% non-fat milk and incubated 1h or overnight with each antibody, washed extensively and incubated for 5 min with Clarity Western ECL Substrate (BioRad). The chemiluminescence signal was acquired using a ChemiDoc Imaging System and the quantification was realized with the ImageLab software (BioRad).

FLIM (Fluorescence Lifetime imaging microscopy)

The pMSCV-mCherry-Syk plasmid (Addgene no. 50045) was used to express via a retrovirus mCherry-Syk in DC2.4 expressing the FcγRI-GFP. For retrovirus production 10^7 HEK-293-FT cells (Invitrogen), at 80% confluence, were transfected with a plasmid mix containing 10 μg of pMSCV-mCherry-Syk plasmid and 10 μg pCL-Ampho plasmid (Novusbio NBP2-29541) in 2.5 mL of transfection buffer (0.125M $CaCl_2$, 25mM BES, 140mM NaCl, 0.75mM Na_2HPO_4). Retroviral supernatant was collected at 24 and 48 h and used directly to transduce DC2.4 cells. Two days later, the cells were selected in puromycin and cloned by limiting dilutions.

The FcγRI-GFP receptors were aggregated using the same protocol as for the co-immunoprecipitation experiments. After the removal of the unbound antibodies, the cells were shifted to 37°C for the different time points of the assays, fixed and analyzed for FRET measurements. Images were acquired on a **TCS SMD FLIM Leica** SP8 confocal microscope and SMD PicoQuant. Image treatment and analysis were performed with Software Symphotime.

ELISA

Mice were injected intraperitoneally with 3% thioglycolate in 1 mL of PBS. Four days later, peritoneal MFs were recovered by peritoneal lavage performed with cold PBS. After red blood cell lysis with ACK lysis buffer, MFs were isolated using Macrophage Isolation Kit from Miltenyi Biotech (ref. 130-110-435) and MF purity was checked by flow cytometry using CD64 and F4/80 staining.

To cross-link FcγRI, MFs were incubated with 5 μg/mL of a rat anti-mouse CD64 (Biorad, AT152-9) for 15 min on ice. Cells were washed 2 times in PBS and incubated 15 min more on ice with 5 μg/mL of a donkey anti-rat (Jackson Immuno-Research). Cells were washed 2 times in PBS and resuspended in RPMI medium containing low IgG serum (Gibco, A33819-01), 2% PS and L-glutamine. For LPS condition, LPS (LPS-B5 from Invivogen) was added in the medium at 100 pg/mL 25 000 cells in 200 μL per well were put into 96 wells plate and incubate for 24 h at 37°C, 5% CO2. Supernatants were then collected and cytokine concentration was measured using mouse ELISA kits from Biolegend (ref. 431603 (IL-12/IL-23 p40) and 431304 (IL-6)).

ADCC

Wt and IRAP-deficient mice were injected intra-peritoneally with 1 mL of 3.8% thioglycolate medium and the peritoneal cells were harvested 72 h later using cold PBS. The MF number was estimated by flow cytometry using the F4/80 antibody and plated on 24 wells plates at 0.2 x10^6 F4/80+ cells per well. Sixteen hours later 0.1 x10^6 HUCCT1 cells were added to each well in the presence of increasing concentrations of anti-EGFR antibody (mouse IgG2a, clone 528, Invitrogen). Three days later, the cells were stained with F4/80-APC and anti-EGFR antibody (mouse IgG1, clone 225, ThermoFisher Scientific), followed by goat F(ab')2 anti-mouse IgG1-FITC (Southern Biotech). The percentage of live HUCCT1 cells was estimated by flow cytometry, as $EGFR^+F4/80^-$ cells.

FcR internalization and IC recycling

FcγRs on WT and IRAP KO BM-DCs were cross-linked with mouse IgG and with a donkey anti-mouse AF488 at 4°C. Then, cells were shifted at 37°C for the indicated time points. At the end, cells were shifted at 4°C and cell surface remaining FcγRI was revealed by fluorescent anti- FcγRI-PE (clone X54-5/7.1) antibodies, while cell surface remaining IC were revealed by a goat anti-donkey DyeLight650.

QUANTIFICATION AND STATISTICAL ANALYSIS

Information about the number of experiments performed are included in figure legends. Values are expressed as mean ± SEM. Statistical significance between two groups was analyzed using the unpaired Student's *t* test, p values are indicated as: *$p < 0.05$; **$p < 0.01$; ***$p < 0.001$; ****$p < 0.0001$. GraphPad Prism version 7.0 was used to perform the statistical analysis.